# Planar Asymmetric Lipid Bilayers of Glycosphingolipid or Lipopolysaccharide on One Side and Phospholipids on the Other: Membrane Potential, Porin Function, and Complement Activation

Andre Wiese,* Jan O. Reiners,* Klaus Brandenburg,* Kazuyoshi Kawahara,‡ Ulrich Zähringer,* and Ulrich Seydel*

*Forschungsinstitut Borstel, D-23845 Borstel, Germany, and ‡Department of Bacteriology, The Kitasato Institute, Tokyo 108, Japan

ABSTRACT   We have determined some physicochemical properties of the monosaccharide-type fraction (GSL-1) of glycosphingolipids, the major glycolipid components of the outer leaflet of the Gram-negative species *Sphingomonas paucimobilis*. These properties included the state of order of the hydrocarbon moiety, the effective molecular area, surface charge density, and intrinsic transmembrane potential profile of reconstituted planar asymmetric GSL-1/phospholipid bilayer membranes. We have, furthermore, investigated the insertion into and the function of porin channels in the reconstituted bilayers and the complement-activating capability of GSL-1 surfaces. All results were compared with respective data for deep rough mutant lipopolysaccharide of *Salmonella minnesota* R595. We found a remarkable agreement in most functional properties of the two glycolipids.

## INTRODUCTION

The cell envelope of Gram-negative bacteria is composed of the cytoplasmic membrane, the peptidoglycan layer, and the outer membrane, which represents an additional permeation barrier and which is strictly asymmetric with respect to its lipid composition. Whereas the inner leaflet of the outer membrane contains only phospholipids, the outer leaflet is usually composed of lipopolysaccharides (LPS), which consist of an oligo- or polysaccharide moiety and a covalently linked lipid component, termed lipid A, anchoring the LPS in the outer membrane (Rietschel et al., 1994). The outer membrane represents a molecular sieve allowing hydrophilic substrates to permeate through particular pores formed by special outer membrane proteins, the porins (Nakae, 1976). The porin pores are usually formed by three monomeric subunits, each having a molecular weight between 30,000 and 50,000 (Benz et al., 1985; Mauro et al., 1988).

It was found in earlier studies that for the strictly aerobic Gram-negative rod *Sphingomonas paucimobilis* (formerly named *Flavobacterium devorans* (Yamamoto et al., 1978) and *Pseudomonas paucimobilis* (Kawahara et al., 1982)), the attempt to extract an LPS by the phenol/water (Westphal et al., 1952) or the phenol/chloroform/petrol ether method (Galanos et al., 1969) was not successful (Kawahara et al., 1982). Instead, a glycolipid with unexpected and unusual structural features was obtained. This "lipid A-type" glycolipid carried the expected D-glucosamine; however, (R)-3-hydroxylated fatty acid residues were absent. Kawahara et al. (1991) succeeded in the elucidation of the complete

chemical structure of this glycolipid, which is a glycosphingolipid (GSL): the hydrophobic portion was found to be heterogeneous with respect to the dihydrosphingosine residue but was, in any case, quantitatively substituted by a (S)-2-hydroxymyristic acid in amide linkage. The oligosaccharide portion of the two main fractions, GSL-4A and GSL-1, consists of a Man-Gal-GlcN-GlcA tetrasaccharide and a GlcA monosaccharide, respectively.

It is well known that many physicochemical and immunological properties of biological membranes are based on the lipid composition and their distribution over the two membrane leaflets. Thus, the distribution of electric charges across the membrane plays a crucial role in many membrane-related processes, from binding of charged species over insertion and orientation of integral membrane proteins to membrane transport phenomena like carrier transport and voltage-dependent gating of porin channels (Seydel et al., 1992; Wiese et al., 1994). The intrinsic membrane potential is made up of contributions from fixed electrostatic surface charges (Gouy-Chapman potential) and the localization and orientation of electric dipoles (e.g., water molecules) within the headgroups along the bilayer normal. These membrane potentials can be probed with carrier-ion complexes via the measurement of current/voltage ($I/U$) characteristics.

In analogy to recent investigations into the influence of the lipid matrix on the channel properties of LPS-free porin from *Paracoccus denitrificans* (Wiese et al., 1994), in which the role of LPS was emphasized, in the present paper these investigations have been extended to the influence of GSL on porin insertion and function.

We could show with planar asymmetric LPS/PL bilayers that an LPS surface can activate the complement system via the classical pathway (Schröder et al., 1990). The activation results in the formation of membrane attack complexes from C5b-8 monomers binding to the membrane surface and inserting a variable number of C9 monomers into the mem-

brane to form complement pores. Of particular interest is, therefore, the question whether the described mechanism can also be observed with membranes composed of GSL instead of LPS on one leaflet.

To compare the functional roles of the two major amphiphilic components of the outer leaflet of the outer membrane of Gram-negative bacteria, GSL and LPS, for the functions outlined above we have reconstituted the lipid matrix of the outer membrane as a planar asymmetric bilayer, one leaflet of which is composed exclusively of GSL (or LPS, respectively) the other of the natural phospholipid mixture resembling the composition of the inner leaflet of the bacterial outer membrane. With these reconstitution systems we could, via electrical measurements of membrane conductivity (current), obtain information on such properties as membrane potential, porin incorporation, and complement activation. These studies were complemented by measurements of the fluidity of pure GSL-membrane systems with fluorescence polarization and Fourier-transform infrared (FTIR) spectroscopy and of the molecular area of GSL molecules arranged in monolayers at the air-water interface with a film balance. The present investigations were restricted to the glycosphingolipid with the shortest sugar moiety, GSL-1, and deep rough mutant LPS Re of *Salmonella minnesota* mutant strain R595.

## MATERIALS AND METHODS

### Lipids and other chemicals

The glycosphingolipid GSL-1 was extracted from *S. paucimobilis* IAM12576 with chloroform/methanol (Kawahara et al., 1991) and successively eluted from a silica gel column by stepwise increase in methanol content. LPS was not present in these preparations, as was confirmed chemically by the lack of 3-OH fatty acids. In Fig. 1, the chemical structure of GSL-1 is depicted, showing that the hydrophobic part is heterogeneous with respect to the occurrence of two different sphingosine derivatives (*erythro*-1,3-dihydroxy-2-amino-octadecane and *erythro*-1,3-dihydroxy-2-amino-*cis*-13,14-methylene-eicosane), which are present in a ratio of 1:4.

Deep rough mutant LPS of *S. minnesota* mutant strain R595 (for the chemical structure see Fig. 1) was used in experiments with asymmetric LPS/PL membranes. LPS was extracted by the phenol/chloroform/petroleum ether method (Galanos et al., 1969), purified and lyophilized, and used in its natural salt form.

Phosphatidylcholine (PC) from egg yolk (type XI-E), phosphatidylethanolamine (PE) from bovine brain (type I), phosphatidylglycerol (PG) from egg yolk lecithin (sodium salt), and diphosphatidylglycerol (DPG) from bovine heart (sodium salt) were purchased from Sigma (Deisenhofen, Germany) and used without further purification. Phospholipids (2.5 mg/ml) were dissolved in chloroform, GSL-1 (1.0 mg/ml) in chloroform/methanol (10:1 v/v) at room temperature, and LPS Re (2.0 mg/ml) in chloroform/methanol (10:1 v/v) and heated to 80°C for 5 min.

The K$^+$ carrier nonactin and whole human serum (WHS) were from Sigma.

LPS-free porin from *Paracoccus denitrificans* ATCC 13543 was a generous gift of W. Welte (Universität Freiburg, Germany) and was prepared as described in detail by Wiese et al. (1994).

### Preparation of planar bilayers and measurements

The planar bilayers were prepared according to the Montal-Mueller technique (Montal and Mueller, 1972). The apparatus for membrane formation consisted of two teflon compartments of 1.5 ml volume each, which were separated by a teflon septum (12.5 $\mu$m thick) with a small aperture (typically 150 $\mu$m diameter). Before membrane formation, the septum was pretreated with a hexan/hexadecan mixture (20:1 v/v). Membranes were formed by apposing the two lipid monolayers, each spread on aqueous subphases, over the aperture. For the reconstitution of the outer membrane of *S. paucimobilis* we used GSL-1 corresponding to the outer leaflet and a lipid mixture composed of PE, PG, and DPG (cardiolipin) in a molar ratio of 81:17:2 corresponding to the PL leaflet. This composition was found to be typical for the phospholipid content of Gram-negative bacteria like *Salmonella typhimurium* (Osborn et al., 1972). For electrical measurements, planar membranes were voltage-clamped via a pair of Ag/AgCl electrodes (type IVM E255; Zak GmbH, Simbach, Germany), which were connected with the headstage of a BLM 120 bilayer membrane amplifier (Biologic, Claix, France) with a feedback resistor of 1 G$\Omega$. For the conductance measurements, a voltage was applied to one electrode (*cis* compartment), and the other (*trans* compartment) was grounded. The carrier measurements were made with a separate experimental setup in which the *cis* compartment was grounded. The potential could be varied in steps of 1 mV by a built-in power supply or continuously via an external control voltage. The latter was connected to the membrane amplifier from
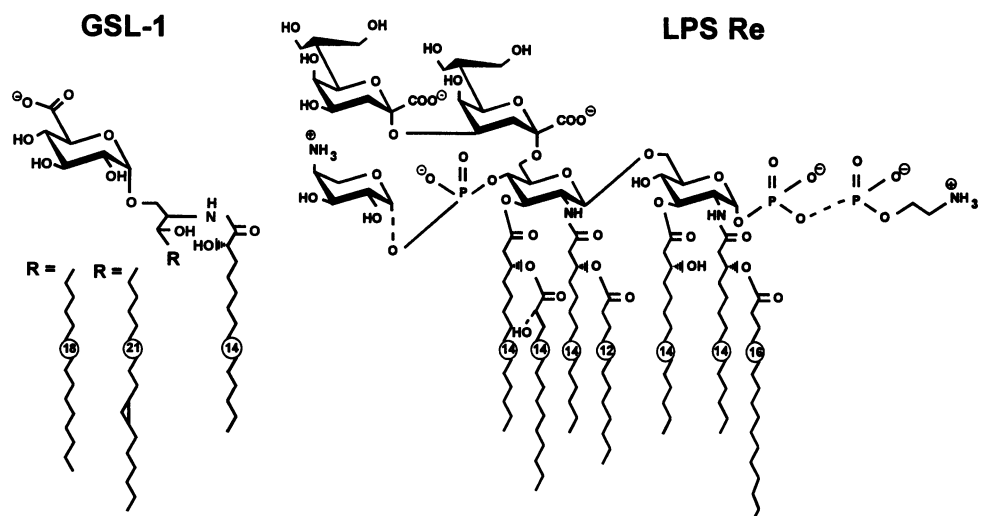


**GSL-1** **LPS Re**

FIGURE 1 Chemical structures of the monosaccharide-type glycosphingolipid GSL-1 from *Sphingomonas paucimobilis* IAM 12576 (*left*) and of deep rough mutant LPS Re from *Salmonella minnesota* R595 (*right*). The dashed lines indicate nonstoichiometric substitutions.

an analog output card PCI 20093-W (Intelligent Instrumentation, Leinfelden, Germany) plugged into an AT-compatible microcomputer system. Membrane current and holding voltage were stored using a DAT tape recorder (DTR 1200, Biologic). The stored signals were sent to the microcomputer system filtered by a 4-pole low-pass Bessel filter (Ithaco Scientific Instruments, Ithaca, NY), the corner of which was adjusted to 10 Hz ($-3$ dB) and digitized at a sampling rate of 10 Hz with a PCI 20089W-1 analog input board (Intelligent Instrumentation). Current was positive when cation flux was directed toward the grounded compartment.

The carrier transport measurements were performed with a subphase consisting of 50 mM KCl, 5 mM MgCl$_2$, and 5 mM HEPES buffer at pH 7.4. Nonactin (final concentration of $10^{-5}$ M) was added to both compartments before membrane preparation.

For incorporation of porins, different concentrations were diluted in an aqueous solution containing 150 $\mu$g/ml Triton X-100 to give a final concentration of 5 ng/ml. Porin was added to the PL side of the bilayer, which was grounded (*trans* compartment), and the subphase (the same as above except for 100 mM KCl instead of 50 mM) was stirred for 30 s before measurement.

For complement activation, WHS was added to the GSL-1 or LPS Re side, which were facing the *cis* compartment. All sera and complement compounds were thawed directly before measurement and diluted to give a final concentration of 1:300 in a subphase consisting of 100 mM KCl, 5 mM MgCl$_2$, and 5 mM HEPES buffer at pH 7.4.

All measurements were performed at a subphase temperature of 37°C.

## FTIR spectroscopic measurements

FTIR spectroscopy was applied for the determinations of the phase behavior of LPS Re and GSL-1 and of the pK value of GSL-1. The measurements were performed on a Nicolet 5-DX (Nicolet Instruments, Madison, WI) by accumulating 50 interferograms, apodizing with a Happ-Ganzel function, Fourier transformation, and conversion to absorbance spectra.

For the measurement of the $\beta \leftrightarrow \alpha$ phase transition behavior, 10 $\mu$l of a $10^{-2}$ M aqueous solution was dispersed directly between two CaF$_2$ windows separated by a 12.5-$\mu$m teflon spacer, and spectra were recorded every 3°C in the temperature range 10°C to 60°C (Casal and Mantsch, 1984; Brandenburg and Seydel, 1990). The peak position of the symmetric stretching vibration of the methylene groups $\nu_s(CH_2)$ at 2850 cm$^{-1}$ was taken as measure of the state of order of the acyl chains.

For the determination of the pK value, a $5 \times 10^{-2}$ M solution of GSL-1 in HEPES buffer in a pH range between 3 and 12 was prepared as above, and the ratio of the peak intensities of the symmetric stretching vibration $\nu_s(COO^-)$ at 1415 cm$^{-1}$ and the pH-independent amide vibration at 1650 cm$^{-1}$ was evaluated for dependence on pH. Below the pK value this ratio is low because of the protonation of the negative charge, and above it is high. From the thus determined pK value, the number of negative charges of GSL-1 at pH 7.4 was calculated.

## Fluorescence polarization

Fluorescence polarization spectroscopy was used as a second independent method for the determination of the $\beta \leftrightarrow \alpha$ phase transition. In this technique, the state of order of the acyl chains is monitored via the hydrophobic fluorescence label diphenylhexatriene (DPH). For this, a $10^{-3}$ M lipid suspension is labeled with $10^{-5}$ M DPH. The dye is excited by polarized light at 360 nm, and the intensities of the emission light at 430 nm are measured simultaneously parallel ($I_{\parallel}$) and perpendicular ($I_{\perp}$) to the polarization plane of the incident beam. Measurements were performed on the fluorescence spectrometer SPEX F1T11 (SPEX Instruments, Edison, NY). The calculation of the fluorescence polarization $P$ was performed according to the relation $P = (I_{\parallel} - I_{\perp})/(I_{\parallel} + I_{\perp})$. $P$ was measured as function of temperature in the range 10°C to 60°C at a heating rate of 1°C/min.

## Film balance measurements

Pressure-area isotherms were obtained with a thermostated Langmuir film balance equipped with a Wilhelmy system. Monolayers were spread from $10^{-3}$ M chloroform/methanol (9:1 v/v) solutions of GSL-1 and LPS Re, respectively, on an aqueous subphase containing 50 mM KCl, 5 mM MgCl$_2$ in HEPES buffer at pH 7.4. The experiments were run at 37°C. Before isotherm registration, monolayers were equilibrated at zero pressure for 5 min to allow evaporation of the solvent, compressed to 15 mN m$^{-1}$, and allowed to equilibrate for 15 min. After that, the monolayers were expanded to zero pressure and allowed to equilibrate for 10 min, and the area-pressure isotherms were registered at a compression rate of 0.1 mm s$^{-1}$. The molecular areas of GSL-1 and LPS Re, respectively, were then determined at a surface pressure of 30 mN m$^{-1}$.

## RESULTS

### Phase behavior

The characteristics of a biological membrane as a permeation barrier depend on, among other things, the fluidity (state of order) of the hydrocarbon chains of the constituing lipid molecules. Furthermore, a relatively high fluidity (low state of order of GSL-1 or LPS Re) is a prerequisite for the preparation of stable asymmetric bilayers. To determine the state of order of GSL-1 and LPS Re, we have performed fluorescence polarization measurements with the fluorophore DPH and FTIR spectroscopic measurements. In Fig. 2, the fluorescence polarization $P$ and the peak position of the symmetric stretching vibration of the methylene groups $\nu_s(CH_2)$, respectively, are plotted versus temperature for GSL-1 and compared with the respective data for LPS Re. Clearly, LPS Re has a highly ordered gel phase at low temperatures ($P$-values around 0.4 and wavenumbers around 2850 cm$^{-1}$, respectively) and undergoes a sharp phase transition at $T_C \approx 31$°C, whereas GSL-1 shows a continuously decreasing state of order (continuously decreasing $P$-values and increasing wavenumbers) over the entire temperature range. Most interestingly, however, is the
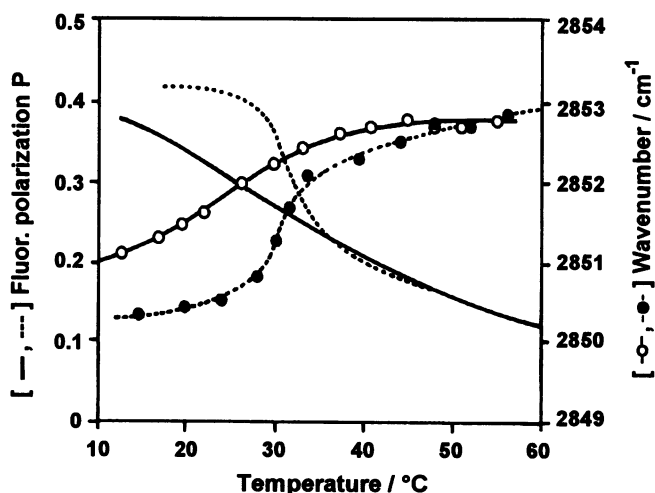


FIGURE 2  Fluorescence polarization and peak position of the symmetric stretching vibration $\nu_s(CH_2)$ in dependence on temperature for GSL-1 (*solid lines*) and LPS Re (*dotted lines*).

fact that the respective states of order for GSL-1 and LPS Re are nearly identical at the physiological temperature of 37°C. Both glycolipids have, however, a significantly higher state of order at 37°C than the PL mixture of the inner leaflet (data not shown).

## Film balance measurements

To determine the effective areas of the GSL-1 and LPS Re molecules in a monolayer at a physiological lateral pressure, we have performed film balance measurements with monolayers spread from chloroform/methanol solutions of these glycolipids on an aqueous subphase. The molecular areas at a surface pressure of 30 mN m$^{-1}$ are 0.37 nm$^2$ for GSL-1 and 1.35 nm$^2$ for LPS Re from $S.$ $minnesota$ R595, respectively (Fig. 3).

These data are important for the calculation of the respective surface charge densities of monolayers made from GSL-1 or LPS Re (see next section).

## Membrane potential

Lipid asymmetry, in particular with respect to surface charge density, may cause a potential difference between the two surfaces of the bilayer membrane, the so-called intrinsic membrane potential. Extreme asymmetries in charge density as well as in headgroup conformation occur in glycolipid/PL bilayers like GSL/PL or LPS/PL. At pH 7.4 of the subphase, LPS Re carries approximately 4.5 negative charges per molecule; thus the resulting surface charge density would be 3.33 elementary charges/nm$^2$, corresponding to $-0.53$ As/m$^2$. For GSL-1 the number of negative charges was determined from FTIR measurements of the pK value as 0.5 per molecule; thus a value of 1.35 elementary charges/nm$^2$ or $-0.22$ As/m$^2$, respectively, was calculated. Within the PL monolayer, at neutral pH the PG molecules

carry one and the DPG molecules two negative charges each. The molar concentrations of PG and DPG in the natural PL mixture are 17% and 2% and the areas per molecule are 0.6 nm$^2$ and 1.1 nm$^2$ (unpublished results), respectively. Thus, the resulting surface charge density of the PL monolayer is approximately 0.31 elementary charges/nm$^2$ or $-0.05$ As/m$^2$.

The surface charge density of a lipid layer results in a surface potential, which can be estimated from the Gouy equation (McLaughlin, 1989):

$$U_{GC} = \frac{2kT}{Ze_0} a \sinh \frac{\sigma}{(8\epsilon\epsilon_0 kTN_A c)^{1/2}} \qquad (1)$$

where $k$ is the Boltzmann constant, $T$ the absolute temperature, $\epsilon$ the relative dielectric number of the subphase, $\epsilon_0$ the dielectric constant, $e_0$ the elementary charge, $Z$ the valence of the counter-ions, $c$ the concentration of the subphase, $N_A$ Avogadro's number, and $\sigma$ the surface charge density (all in SI units). Instead of the concentration, frequently the ionic strength is used.

The thus calculated values for the GSL-1, LPS Re, and the PL layers are given in Table 1.

The potential profile across the various bilayers was probed with the K$^+$ carrier nonactin via the registration of $I/U$ characteristics. The $I/U$ curves were evaluated according to procedures described previously (Seydel et al., 1992). Briefly, the current $I$ as function of the voltage $U$ applied with the voltage clamp is given by Schoch et al. (1979):

$$I_m = K \frac{(\Delta\Phi + (n_2 - n_1) U)}{(n_2 - n_1)} \cdot \frac{e^{aU} - 1}{e^{a \cdot (\Delta\Phi + n_2 U)} - e^{an_1 U}} \qquad (2)$$

where $a = (Z \cdot e_0)/(k \cdot T)$, $K$ is a constant for each membrane (depending on, among other things, its area and thickness), $n_1$, $n_2$ are the edges of the potential walls for the two leaflets, and $\Delta\Phi$ is the potential difference between these edges. The three parameters describe the shape of the trapezoidal energy barrier and were determined from the experimental curves by computer fitting of the above equation.

In Fig. 4, $I/U$ characteristics for asymmetric planar GSL-1/PL (left) and LPS Re/PL (right) bilayers are given together with the respective fits according to Eq. 2. Clearly, both characteristics are asymmetric. In both cases, the fits for the $I/U$ curves are ideal, such that the measured data can
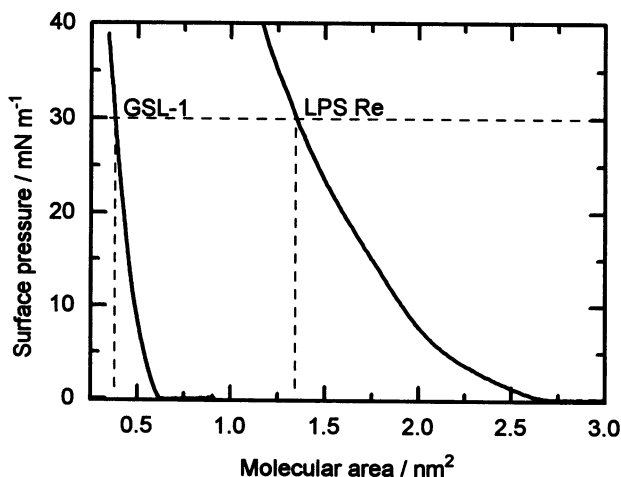


FIGURE 3  Pressure-area isotherms of monolayers spread from chloroform/methanol solutions (90:10 v/v) of GSL-1 and LPS Re. Subphase: 50 mM KCl, 5 mM MgCl$_2$, 5 mM HEPES buffer at pH 7.4; $T = 37$°C.

TABLE 1  Molecular area, molecular charge, and surface potential according to the Gouy equation for GSL-1, LPS Re, and PL calculated for a 5 mM HEPES subphase at pH 7.4 containing 50 mM KCl and 5 mM MgCl$_2$ (resulting ionic strength of the subphase: 65 mM) and a subphase temperature of 37°C

|        | Area/molecule, nm$^2$ | Charge/molecule, $e_0$ | Surface potential, mV |
|--------|------------------------|--------------------------|------------------------|
| GSL-1  | 0.37                   | $-0.5$                   | $-144$                 |
| LPS Re | 1.35                   | $-4.5$                   | $-191$                 |
| PL     | 0.60                   | $-0.17$                  | $-69$                  |

FIGURE 4 I/U characteristics of nonactin-doped asymmetric GSL-1/PL (left) and LPS Re/PL (right) bilayer membranes. Subphase: 50 mM KCl, 5 mM MgCl₂, 5 mM HEPES buffer at pH 7.4; subphase temperature 37°C; maximal membrane current was normalized to 1. The fits (dotted lines) were calculated according to Eq. 2.
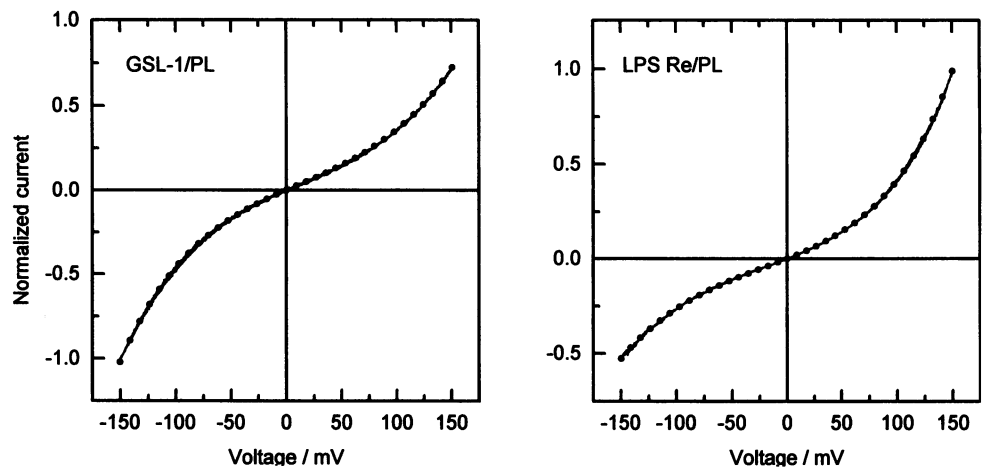
be completely superimposed. The values for the parameters $n_1$ and $n_2$ are 0.21 and 0.79 for GSL-1 and 0.22 and 0.78 for LPS Re, and the potential differences $\Delta\Phi$ are 20 mV and −38 mV, respectively.

The calculated intrinsic membrane potential profiles for the two bilayer systems are plotted in Fig. 5, reflecting the differences in the respective Gouy-Chapman potentials of the glycolipid leaflets and in the contributions of the dipole potentials. The latter is expressed in the sign as well as in the absolute height of the potential difference $\Delta\Phi$.

## Incorporation and function of porins

Addition of 5 ng/ml porin of *P. denitrificans* to the PL side of asymmetric GSL-1/PL bilayers led to a rapid increase of membrane current, which decelerated typically after some minutes. Porin channels did not incorporate at all when added to the GSL-1 side. The incorporation rate of porins into asymmetric GSL-1/PL bilayers is of a magnitude similar to that of the incorporation rate into LPS Re/PL membranes, and in both systems the incorporation rate is higher by an order of magnitude than that into a symmetric PL membrane (Fig. 6).

At lower porin concentrations and low clamp voltages (10–20 mV), stepwise current increase could be observed. From these current traces, single-channel conductance was derived. By comparing the single-channel conductance of

porins in asymmetric LPS Re/PL bilayers with that in symmetric PL membranes we could already rule out an effect of the lipid matrix on this parameter (Wiese et al., 1994). We have now extended these investigations on the asymmetric GSL-1/PL lipid matrix. The results for single-channel conductance of porins of *P. denitrificans* in that lipid environment are compared to those in LPS Re/PL membranes in Fig. 7. Obviously, the mean value of the single-channel conductance is identical in the two membrane systems, $\Lambda = (0.43 \pm 0.03)$ nS for GSL-1/PL bilayers and $\Lambda = (0.44 \pm 0.05)$ nS for LPS Re/PL bilayers, respectively. From these mean single-channel conductivities, mean effective pore diameters could be estimated as $d = 1.5$ nm ($\Lambda = \pi\sigma d^2/4l$; $\sigma$ is the specific conductance of the subphase; $l$ is the length of the pore corresponding to membrane thickness).

Porin channels reconstituted in asymmetric GSL-1/PL membranes showed voltage-dependent activity. Similar observations have been made in other membrane systems. At sufficiently high clamp voltages, channel closing was observed. To compare the amplitude of the voltage necessary for channel gating, we have measured I/U curves for the two membrane systems GSL-1/PL and LPS Re/PL. Voltage ramps (4 mV s⁻¹) were driven when (after addition of 5 ng/ml porin to the PL side) porin incorporation had decelerated or even stopped. In both membrane systems, the recorded traces exhibited a hysteretic behavior (Fig. 8). Going from zero voltage in either direction to approxi-



FIGURE 5 Intrinsic membrane potential profiles for GSL-1/PL (left) and LPS Re/PL (right) bilayer membranes. The Gouy-Chapman potentials were obtained from Eq. 1, and the trapezoidal inner membrane potential profiles were calculated from the respective fits of Eq. 2 to the experimental data.
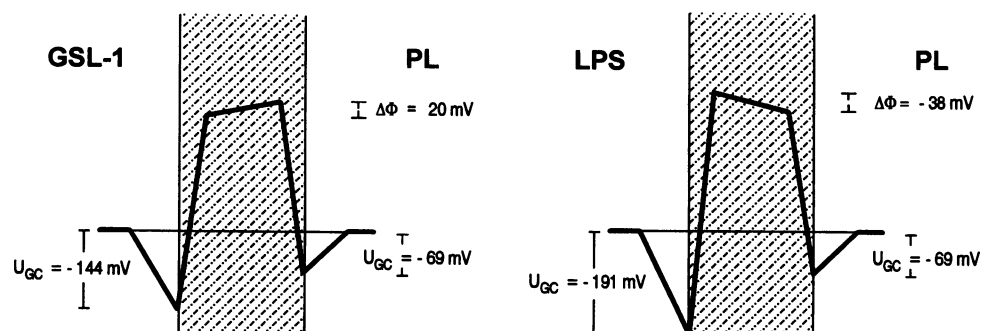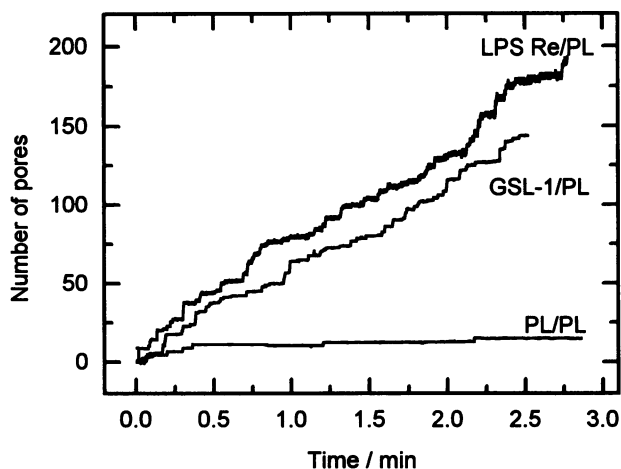
FIGURE 6 Incorporation rates for LPS-free porin (5 ng/ml) from *P. denitrificans* into asymmetric GSL-1/PL and LPS Re/PL and symmetric PL bilayer membranes, respectively. Porin was added to the PL side of the bilayers. Subphase: 100 mM KCl, 10 mM MgCl₂, 5 mM HEPES buffer, pH 6.5; $T$ = 37°C.

mately +100 mV or −100 mV, the measured membrane current changed proportionally to the applied voltage. Above (below) this range, an underproportional increase (decrease), a steady state, or a decrease (increase) in membrane current was observed with increasing (decreasing) voltage. The asymmetry in the shape of the recorded $I/U$ curves, i.e., the voltage at which channel closing started and the area of the hysteresis slopes, depended on the asymmetry in the charge densities of the membrane leaflets.

## Complement activation

We have performed first experiments with GSL-1/PL bilayers to find out whether GSL surfaces have complement-activating capabilities. Fig. 9 shows the macroscopic conductance changes in dependence on time after the addition of WHS (dilution, 1:300) to the subphase (100 mM KCl, 5 mM MgCl₂, 5 mM HEPES buffer, pH 7.4) at the GSL-1

side of an asymmetric GSL-1/PL bilayer. Clearly, membrane conductance increases significantly with time.

At higher dilutions of WHS, microscopic traces were obtained showing a stepwise increase that can be resolved at the beginning of complement pore formation. An example is given in Fig. 10. From the evaluation of a larger number of similar experiments, the mean single-step conductance was determined to be 0.41 ± 0.06 nS; however, a second population was also observed at twice this value. The amplitude distribution of the single-step conductance is also given in Fig. 10.

Addition of WHS to the PL side of the bilayer system, even at higher concentrations than above, did not induce any conductance changes within an observation period of up to 30 min.

## DISCUSSION

The outer leaflet of the outer membrane of the Gram-negative bacterial species *S. paucimobilis* has been shown to be composed of glycosphingolipids instead of lipopolysaccharides (Kawasaki et al., 1994). Like lipopolysaccharides, glycosphingolipids consist of a lipid anchor to which a sugar moiety is covalently linked. The lipid anchor is made up by dihydrosphingosine, which is substituted by 2-hydroxymyristic acid in amide linkage, and the sugar portion expresses, as in LPS, a variation in its length. The structure with the shortest sugar moiety, a glucuronic acid, is termed GSL-1; that with the longest sugar portion known so far, carrying three additional sugars, is termed GSL-4A. Because the glycosphingolipid was shown to be localized at the cell envelope with the antigenic sugar portion exposed on the bacterial cell surface, the question arose whether the functions of glycosphingolipids were similar to those of the lipopolysaccharide of other Gram-negative bacteria. We have, therefore, in a first step determined some physicochemical properties of GSL-1, including the state of order (fluidity) of its hydrocarbon moiety, the effective molecular area, the surface charge density, and the intrinsic membrane potential of a GSL-1/PL bilayer. We have, furthermore,
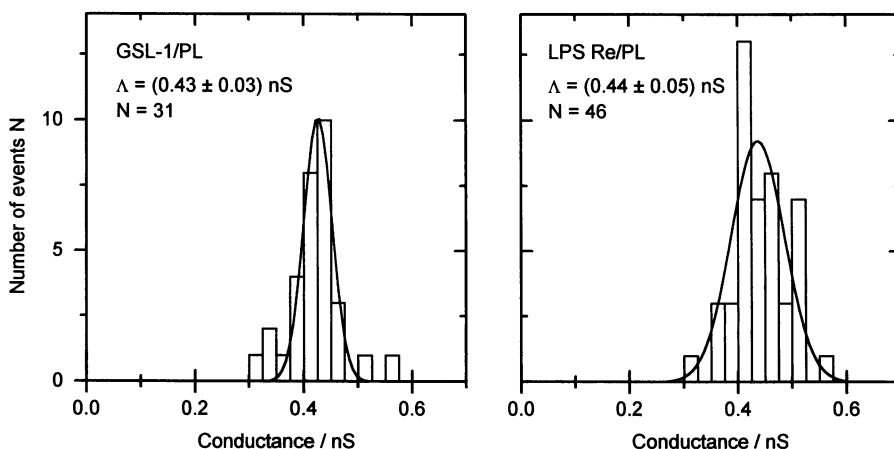


FIGURE 7 Histograms of the amplitudes of the conductance steps of GSL-/PL (*left*) and LPS Re/PL (*right*) bilayer membranes and derived single-channel conductances after addition of 10 pg/ml porin. Subphase: 100 mM KCl, 10 mM MgCl₂, 5 mM HEPES buffer, pH 6.5; $T$ = 37°C.

FIGURE 8 *I/U* curves of porin-doped GSL-1/PL (*left*) and LPS Re/PL (*right*) bilayer membranes normalized to the value at 40 mV (i.e., when all channels are open). Subphase: 100 mM KCl, 10 mM MgCl₂, 5 mM HEPES buffer, pH 6.5; $T = 37°C$.
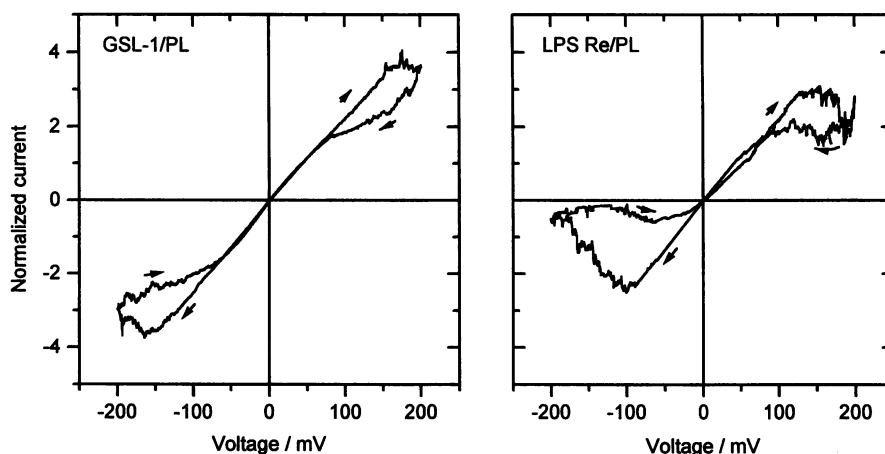
investigated the influence of the GSL-1 matrix on insertion and function of porin channels and its capability to activate the human complement system. All data were compared with respective data from LPS Re from *S. minnesota* R595.

In general, we found a surprising agreement in the above-mentioned properties of GSL-1 and LPS Re. Thus, the fluidities of the hydrocarbon moieties of these two compounds at physiological temperature were nearly identical (Fig. 2). This implies that the permeation properties of the lipid matrices of the outer membranes carrying either GSL-1 or LPS Re are very similar.

The effective molecular areas as determined from pressure-area isotherms of monolayers at the air-water interface at a surface pressure of 30 mN m$^{-1}$ (this value is well within the range of experimentally found or calculated lateral pressures in biological bilayer membranes under physiological conditions) (Marcelja, 1974; Nagle, 1976; Blume, 1979) differ considerably: 0.37 nm² for GSL-1 and 1.35 nm² for LPS Re (Fig. 3). This should not be surprising
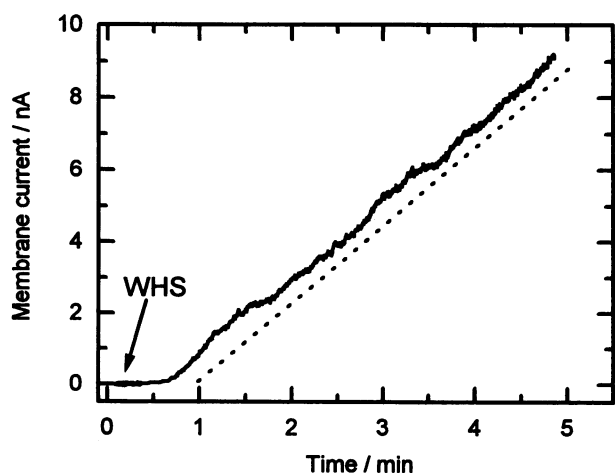


FIGURE 9   Macroscopic current response of an asymmetric GSL-1/PL bilayer membrane upon addition of WHS to the aqueous subphase at the GSL-1 side of the membrane (final dilution of serum, 1:300). Transmembrane voltage was clamped to +20 mV. Subphase: 100 mM KCl, 5 mM MgCl₂, 5 mM HEPES buffer, pH 7.4; $T = 37°C$.

when considering the fact that the number of alkyl chains of the lipid A moiety of LPS is higher by a factor of 3 than that of the lipid portion of GSL. It may be assumed, however, that the surface charge density of the outer leaflet of the outer membrane, rather than the molecular area of the composing glycolipids, is an important parameter for the function of the outer membrane. Thus, an asymmetric potential profile has been observed in membranes with an asymmetric distribution of the surface charge densities on the opposing monolayers (Hall and Latorre, 1976), in membranes with a symmetric distribution of the charge densities but with an asymmetry with respect to the headgroup conformations of the two leaflets (Latorre and Hall, 1976), and in symmetric membranes with asymmetry of the subphases (Schoch et al., 1979). We have calculated the surface charge densities from the effective number of charges of the glycolipid molecules per unit area and arrived at considerably different values, which were 1.35 and 3.33 elementary charges/nm² for GSL-1 and LPS Re, respectively, on the basis of 0.5 negative charges per GSL-1-molecule and 4.5 charges per LPS Re-molecule at pH 7.4.

The surface charge density is an important determinant for the surface potential (Gouy-Chapman potential), which is one component of the intrinsic membrane potential and influences the transmembrane potential profile. A second component is represented by the dipole potential. To determine the overall transmembrane potential, we have registered *I/U* curves from K$^+$/nonactin carrier-complex diffusion through GSL-1/PL and LPS Re/PL membranes, respectively, to which we fitted theoretical curves calculated on the basis of the procedure of Schoch et al. (1979) (Fig. 4). In both cases, the fits were extremely good. The inner trapezoidal transmembrane potential profiles ΔΦ derived from these fits (Fig. 5) show differences in the absolute height as well as in the sign. The Gouy-Chapman potentials of the glycolipid leaflets show also significant differences in their absolute values. The differences in ΔΦ of the two membrane systems result from differences in the contributions of the dipole potentials, which, however, cannot yet be definitely assigned to particular conformational

FIGURE 10 Microscopic current steps (*left*) and histograms of the amplitudes of the conductance steps and derived single-channel conductances of a GSL-/PL bilayer membrane upon addition of WHS to the aqueous subphase at the GSL-1 side of the membrane (final dilution of serum, 1:300). Transmembrane voltage was clamped to +20 mV. Subphase: 100 mM KCl, 5 mM $MgCl_2$, 5 mM HEPES buffer, pH 7.4; $T = 37°C$
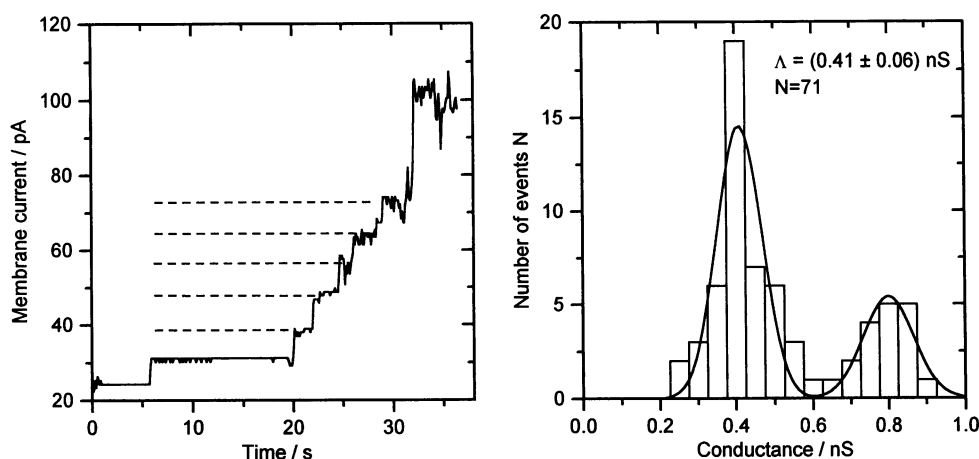
differences in the GSL-1 and LPS Re molecules. Contributions to these differences should arise, however, from the amount and orientation of water molecules in the interface region between membrane surface and water phase and from dipoles within the glycolipids themselves.

The comparison of the incorporation rates and channel properties of LPS-free porin in the two membrane systems proved once more (Wiese et al., 1994) that the lipid matrix does not influence the channel geometry. Thus, the single-channel conductance and hence the size of the porin channel were found to be identical within the experimental error for the GSL-1/PL and the LPS Re/PL bilayer lipid matrices, respectively (Fig. 7). GSL-1 does, however, influence the incorporation rate and the gating behavior, as does LPS Re. The rates of incorporation into pure phospholipid bilayer systems are more than a factor of 10 lower than those into asymmetric membranes with a GSL-1 or LPS Re leaflet on the opposite side (Fig. 6). We could show that the incorporation rate was independent of the surface charge density of the monolayer opposite the side of porin addition and independent of the effective (intrinsic plus applied) membrane potential. As we have discussed previously (Wiese et al., 1994), this observation should be a strong indication for specific interactions between the porin molecules with the GSL or LPS leaflet, respectively and corresponds to the model of Weiss et al. (1991, 1992), who propose that the very polar zone on the outer surface of the β-barrel with its numerous negatively charged residues is directed toward the extracellular medium. The carboxylate groups of the porin, according to these authors, are likely to participate in the strong and tight network of divalent cations and carboxylate groups within the layer of LPS core units in such a way that the interface between these core units and porin would become as tight as the LPS layer itself.

The complete prevention of porin incorporation from the GSL-1 and LPS Re sides may be explained in several ways. Benz et al. (1985) reported on lipid-dependent incorporation rates for *S. typhimurium*, *Escherichia coli*, and *Pseudomonas aeruginosa* porins into black lipid membranes. From these results the author deduced that porins incorporate into

membranes formed by lipids with a smaller headgroup at a higher rate. This hypothesis does not explain, however, the similarity between GSL-1 and LPS Re, which differ by a factor of 3 in their effective molecular areas. Other reasons might be the rigidity of the GSL-1 and LPS Re leaflets (both glycolipids have, at physiological temperature, a higher state of order than most natural phospholipids) or the steric hindrance caused by the sugar moieties of the glycolipids.

We have observed voltage-dependent gating for porin channels in both asymmetric bilayer systems (Fig. 8); however, this occurred at different voltages in the differently composed membranes. In a previous paper (Wiese et al., 1994), in which we also discussed the biological relevance of voltage gating, we correlated the heights of the surface potential on one hand and the shape of the recorded I/U curves on the other for LPS Re/PL bilayers, taking into account the surface charges and the Gouy-Chapman potentials derived therefrom. It is obviously that for GSL-1/PL bilayers for the observed voltage gating a respective correlation can also be stated, considering that (at pH 6.5 of the subphase in these experiments) less than 0.5 negative charges per GSL-1 molecule are present.

We have previously shown (Schröder et al., 1990) that the addition of WHS to the subphase at the LPS side of the asymmetric LPS Re/PL membrane resulted in a rapid increase of the bilayer conductance in discrete steps, indicating the formation of transmembrane pores. The amplitudes of the discrete conductance steps varied over a range of more than one order of magnitude, and the mean single-step conductance was (0.39 ± 0.24) nS for a subphase containing 100 mM KCl, 5 mM $MgCl_2$, and 5 mM HEPES buffer at pH 7.4. The steps were grouped into bursts of typically 9 ± 3 events per burst, and the conductance change within one burst was (8.25 ± 4.00) nS. The pore-forming activity of serum was independent of the presence of specific antibodies against LPS but was dependent on calcium ions, and the pore-forming activity required complement components C1q and C9. From these experimental findings we concluded that activation of complement by LPS Re involves the classical pathway.

The experimental data obtained so far with the GSL-1/PL bilayer system provide clear evidence that the human complement system is activated by a GSL-1 surface (Fig. 9) and that the pore-forming mechanism is similar to that observed with the LPS Re/PL membrane. Thus, pore formation proceeds in discrete steps (Fig. 10), and the single-step conductance is comparable in both systems. From the observed identical amplitudes of single-step conductance within a burst it may be concluded that the insertion of C9 monomers leads to the formation of leaky patches, i.e., membrane lesions that are not completely aligned by protein (Schröder et al., 1990). We have no experimental evidence so far for the formation of cylindrical pores, fully aligned by C9 monomers, which would be expressed by a quadratic increase in single-step conductance. For the observation of a second peak in the histogram of single-step amplitudes with the double value of the single-step conductance we do not yet have a decisive explanation; it may be speculated, however, that a dimerization of C9 monomers before insertion into the membrane may occur.

Our results show that GSL-1 and LPS Re exhibit a high degree of similarity in the investigated parameters and properties, and it may thus be concluded that these two glycolipids are very similar with respect to their function as antigenic surface structures as well as to their contribution to the function of the outer membrane of the respective Gram-negative species as diffusion barrier.

## REFERENCES

Benz, R. 1985. Porin from bacterial and mitochondrial outer membranes. *CRC Crit. Rev. Biochem.* 19:145–190.

Benz, R., A. Schmid, and R. E. W. Hancock. 1985. Ion selectivity of Gram-negative bacterial porins. *J. Bacteriol.* 162:722–727.

Blume, A. 1979. A comparative study of the phase transition of phospholipid bilayers and monolayers. *Biochim. Biophys. Acta.* 557:32–44.

Brandenburg, K., and U. Seydel. 1990. Investigation into the fluidity of lipopolysaccharide and free lipid A membrane systems by Fourier-transform infrared spectroscopy and differential scanning calorimetry. *Eur. J. Biochem.* 191:229–236.

Casal, H. L., and H. H. Mantsch. 1984. Polymorphic phase behaviour of phospholipid membranes studied by infrared spectroscopy. *Biochim. Biophys. Acta.* 779:381–401.

Galanos, C., O. Lüderitz, and O. Westphal. 1969. A new method for the extraction of R lipopolysaccharides. *Eur. J. Biochem.* 9:245–249.

Hall, J. E., and R. Latorre. 1976. Nonactin-$K^+$ complex as a probe for membrane asymmetry. *Biophys. J.* 15:99–103.

Kawahara, K., U. Seydel, M. Matsuura, H. Danbara, E. T. Rietschel, and U. Zähringer. 1991. Chemical structure of glycosphingolipids isolated from *Sphingomonas paucimobilis*. *FEBS Lett.* 292:107–110.

Kawahara, K., K. Uchida, and K. Aida. 1982. Isolation of an unusual "lipid A" type glycolipid from *Pseudomonas paucimobilis*. *Biochim. Biophys. Acta.* 712:571–575.

Kawasaki, S., R. Moriguchi, K. Sekiya, T. Nakai, E. Ono, K. Kume, and K. Kawahara. 1994. The cell envelope structure of the lipopolysaccharide-lacking Gram-negative bacterium *Sphingomonas paucimobilis*. *J. Bacteriol.* 176:284–290.

Latorre, R., and J. E. Hall. 1976. Dipole potential measurements in asymmetric membranes. *Nature.* 254:361–363.

Marcelja, S. 1974. Chain ordering in liquid crystals. II. Structure of bilayer membranes. *Biochim. Biophys. Acta.* 367:165–176.

Mauro, A., M. Blake, and P. Labarca. 1988. Voltage gating of conductance in lipid bilayers induced by porin from outer membrane of *Neisseria gonorrhoeae*. *Proc. Natl. Acad. Sci. USA.* 85:1071–1075.

McLaughlin, S. 1989. The electrostatic properties of membranes. *Annu. Rev. Biophys. Biophys. Chem.* 18:113–136.

Montal, M., and P. Mueller. 1972. Formation of bimolecular membranes from lipid monolayers and a study of their electrical properties. *Proc. Natl. Acad. Sci. USA.* 69:3561–3566.

Nagle, J. F. 1976. Theory of lipid monolayer and bilayer phase transitions: effect of headgroup interactions. *J. Membr. Biol.* 27:233–250.

Nakae, T. 1976. Identification of the outer membrane protein of *E. coli* that produces transmembrane channels in reconstituted vesicle membranes. *Biochem. Biophys. Res. Commun.* 71:877–884.

Osborn, M. J., J. E. Gander, E. Parisi, and J. Carson. 1972. Mechanism and assembly of the outer membrane of *Salmonella typhimurium*. *J. Biol. Chem.* 247:3962–3972.

Rietschel, E. T., T. Kirikae, F. U. Schade, U. Mamat, G. Schmidt, H. Loppnow, A. J. Ulmer, U. Zähringer, U. Seydel, F. Di Padova, M. Schreier, and H. Brade. 1994. Bacterial endotoxin: molecular relationships of structure to activity and function. *FASEB J.* 8:217–225.

Schoch, P., D. F. Sargent, and R. Schwyzer. 1979. Capacitance and conductance as tools for the measurement of asymmetric surface potentials and energy barriers of lipid bilayer membranes. *J. Membr. Biol.* 46:71–89.

Schröder, G., K. Brandenburg, L. Brade, and U. Seydel. 1990. Pore formation by complement in the outer membrane of Gram-negative bacteria studied with asymmetric planar lipopolysaccharide/ phospholipid bilayers. *J. Membr. Biol.* 118:161–170.

Seydel, U., W. Eberstein, G. Schröder, and K. Brandenburg. 1992. Electrostatic potential barrier in asymmetric planar lipopolysaccharide/ phospholipid bilayers probed with the valinomycin-$K^+$ complex. *Z. Naturforsch.* 47c:757–761.

Weiss, M. S., U. Abele, J. Weckesser, W. Welte, E. Schiltz, and G. E. Schulz. 1991. Molecular architecture and electrostatic properties of a bacterial porin. *Science.* 254:1627–1630.

Weiss, M. S., and G. E. Schulz. 1992. Structure of porin refined at 1.8 Å resolution. *J. Mol. Biol.* 227:493–509.

Westphal, O., O. Lüderitz, and F. Bister. 1952. Über die Extraktion von Bakterien mit Phenol/Wasser. *Z. Naturforsch.* 7:148–155.

Wiese, A., G. Schröder, K. Brandenburg, A. Hirsch, W. Welte, and U. Seydel. 1994. Influence of the lipid matrix on incorporation and function of LPS-free porin from *Paracoccus denitrificans*. *Biochim. Biophys. Acta.* 1190:231–242.

Yamamoto, A., I. Yano, M. Masui, and E. Yabuuchi. 1978. Isolation of a novel sphingoglycolipid containing glucuronic acid and 2-hydroxy fatty acid from *Flavobacterium devorans* ATCC 10829. *J. Biochem.* 83: 1213–1216.